Damage evolution and particle retention in metals bombarded by neutral helium particles at the first wall positions in LHD

M. Tokitani, N. Yoshida [a], Y. Ohtawa [b], K. Tokunaga [a], T. Fujiwara [a], M. Miyamoto [c], N. Ashikawa,
S. Masuzaki, M. Shoji, M. Kobayashi, A. Sagara, N. Noda, H. Yamada, A. Komori,
LHD experimental group, S. Nagata [d], B. Tsuchiya [d]

National Institute for Fusion Science, 322-6, Toki, Gifu 509-5292, Japan
[a] Research Institute for Applied Mechanics, Kyushu University, Kasuga, Fukuoka 816-8580, Japan
[b] Interdisciplinary Graduate School of Engineering Sciences, Kyusyu University, Kasuga, Fukuoka 816-8580, Japan
[c] Department of Material Science, Shimane University, Matsue, Shimane 690-8504, Japan
[d] Institute for Materials Research, Tohoku University, Sendai, Miyagi 980-8577, Japan

(Received day month year / Accepted day month year should be centered 10-point type)

Specimens of W, Mo and stainless steel were inserted into the first wall equivalent position by using movable material probe system in LHD, and then, exposed to the several sequential helium discharges. After the exposure, very dense helium bubbles and dislocation loops were confirmed in all specimens from transmission electron microscopy (TEM) observation. It means that the energy of incidence helium particles is sufficiently higher than that of the minimum energy for creating the knock-on damage (E_{min}) in all specimens (e.g. W; E_{min}=0.53keV). Majority of such incidence helium particles to the specimens are energetic neutrals created by charge-exchange (CX) collisions [1]. It is known that helium atoms once injected into metals cause more intensive radiation damages than hydrogen atoms, because they have a strong interaction with lattice defects such as vacancies or dislocation loops. Understanding of the effects of charge exchanged helium particles (CX-helium) to the first wall is important for not only the elucidation of materials degradation but also realization of the high performance plasma operations in future fusion devices.

Keywords: Large Helical Device (LHD), Helium, Charge-exchanged neutrals, Microscopic damage, Transmission Electron Microscopy (TEM)

1. Introduction

The first wall materials of fusion reactors will suffer heavy bombardment of helium particles generated by D-T fusion reaction. Majority of such incidence helium particles are energetic neutrals (CX-neutrals) created by charge-exchange collisions [1]. Helium injection into metals causes serious radiation damages. Strong irradiation effects of helium have been observed in many kinds of metals such as tungsten, molybdenum and stainless steel [2-6].

The Large Helical Device (LHD) is the largest heliotron-type device with super conducting magnetic coils [7]. The first wall panels and divertor plates are made of stainless steel and isotropic graphite, respectively. Stainless steel is the major material in LHD and the graphite area is only about 5 % of the total plasma facing area. It was reported that for helium plasma discharge experiments in the LHD, about half of the inlet helium was trapped in the wall, even after a long helium glow discharge cleaning. Therefore, understanding of the effects of charge exchanged helium (CX-helium) atoms

to the first wall is important for not only the elucidation of materials degradation but also the plasma operations. In the case of steady state operations, behavior of incidence CX-helium atoms to the first wall is much important.

In the present study, microscopic damages in metals generated by CX-helium bombardment were studied, and then, incident flux and energy of CX-helium were evaluated.

Furthermore, to investigate the effect of bombardment of CX-helium on optical reflectivity of Mo mirror, change of optical reflectivity was measured by means of spectrophotometer. Mo is one of the potential candidate of first mirror for plasma diagnosis in future fusion devices [8]. Effects of the hydrogen isotope irradiation on optical properties have been studied extensively [9-11] but not much for the helium irradiation. However, our fundamental study on helium irradiation effects on Mo mirror indicated that radiation damages by helium atoms cause serious degradation of optical reflectivity [12].

2. Experimental procedures

2.1. Material irradiation experiments in LHD

Specimens of Mo and stainless steels mounted on the probe head were placed at the first wall equivalent position by using movable material probe system which installed in LHD, and then, exposed to the NBI + ICRF heated helium discharges. This material probe system makes possible to select desirable plasma discharges and irradiation position by using shutter and vertical movement mechanism. Fig. 1 shows a schematic view of the experimental set up in this study.
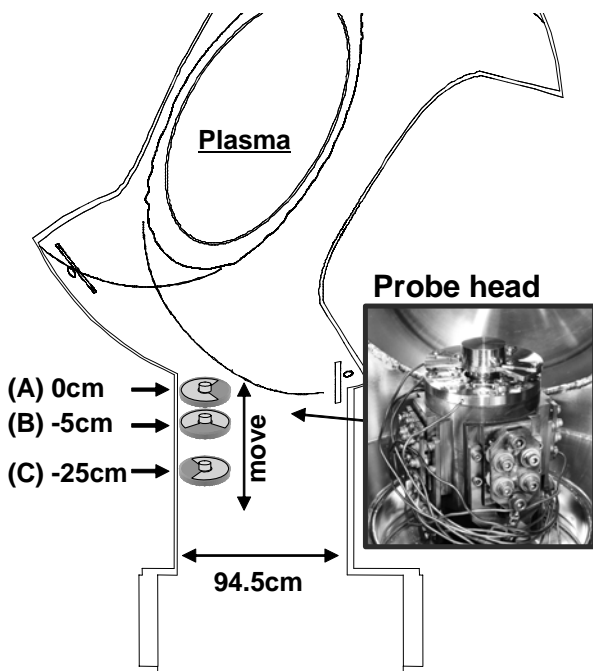
Fig. 1 Schematic view of the experimental set up on movable material probe system in LHD.

Total discharge time at each irradiation position which is identified by the distance measured from the first wall equivalent position and typical plasma parameters summarized in Table 1. For convenience these positions are denoted as (A), (B) and (C). (B) and (C) are the positions in 4.5L port as illustrated in Fig. 1. The temperature of the probe head during exposure was monitored by the thermocouples placed just beneath the specimens. It stayed almost constant near room temperature.

2.2. Material analysis

After the exposure, microscopic damage of the specimens was observed by means of transmission electron microscopy (TEM) and then, incidence flux and energy of CX-helium atoms were estimated by comparing with the in-situ TEM observation results under helium ion-beam irradiation experimental results [13].

Optical reflectivity of Mo mirror before and after the exposure was measured with a spectrophotometer (JASCO, V-670) for the wave length between 190 and 2500 nm.

3. Results and discussions

3.1. Evaluation of microscopic damage by TEM observation

Fig. 2 shows TEM images of (a)-Mo and (b)-stainless steel exposed to the NBI+ICRF heated helium discharges for the case of (A), (C) and (A)+(B)+(C). (A)+(B)+(C) means the specimen exposed at all positions. The upper series of micrographs of (a) and (b) are bright field images with large deviation parameter s. White dot images are helium bubbles. The lower series of (a) and (b) are dark field images with small deviation parameter s, which fits for observation of defects with strong lattice distortion such as dislocation loops and helium platelets. Defects with a strong white image, mainly dislocation loops. Although total irradiation time was only 349 s~1138 s, considerably large amounts of helium bubbles of about 1 to 2 nm and dislocation loops of about ~20 nm were formed in both specimen and all cases. Evolution of the microscopic damage was already saturated at the case of both (A) and (C). Thus, since the creation rate of defects in all specimens was very high, unfortunately, the difference of the damage rate could not identify as a function of irradiation time and position. This means that the damage is caused by CX-helium atoms which are not affected by magnetic field, and their energy and flux are sufficiently higher to create these defects. In general, radiation induced secondary defects are formed as aggregates of point defects produced by knock-on processes. Since the threshold energies of helium for displacement damage in Mo and stainless steel are about

	Distance from first wall position	Total discharge time	Ion temp. T_i (keV) (Plasma core)	Electron density ($\times 10^{19} m^{-3}$)
(A)	0 cm	408 s	0.5~2.0	0.25~3.6
(B)	-5 cm	349 s	0.2~2.0	0.25~2.25
(C)	-25 cm	352 s	0.5~2.0	0.25~3.6
(A)+(B)+(C)		1138 s	0.1~2.5	0.23~3.85

Table 1 Total discharge time at each irradiation distance from the first wall position as illustrated in Fig. 1 and typical plasma parameters. 0 cm corresponds to the first wall equivalent position. (Direction of -25 cm is farthest from plasma)

0.23 keV and 0.10 keV, respectively. The size and density of defects between (A) and (C) were very similar in both specimens. It is indicates that the flux of CX-helium atom does not decrease much even in the port.

3.2. Estimation of the flux and energy of CX-helium atoms

It was tried to estimate the flux and energy of CX-helium atoms to the first walls by comparing with systematic in-situ helium ion irradiation experiments [13]. The microstructural evolution of stainless steel at room temperature under irradiation with 2 keV-He$^+$ ions is shown in Fig. 3. Some of the images are re-produced data from Ref. [13]. The upper series of micrographs are bright field images with large deviation parameter s. The lower series are dark field images with small deviation parameter s. When Fig. 3 compared with Fig. 2-(b), size and density of helium bubbles and dislocation loops of the all cases of Fig. 2-(b) is corresponds to $2\sim5\times10^{21}$ He/m^2. Therefore, the estimated flux and incidence energy is $2\times10^{18}\sim1\times10^{19}$ He/m^{2}s and about $1\sim2$ keV, respectively. As mentioned above, majority of such incidence helium particles are energetic neutrals. This estimation is relatively rough. However, it is important
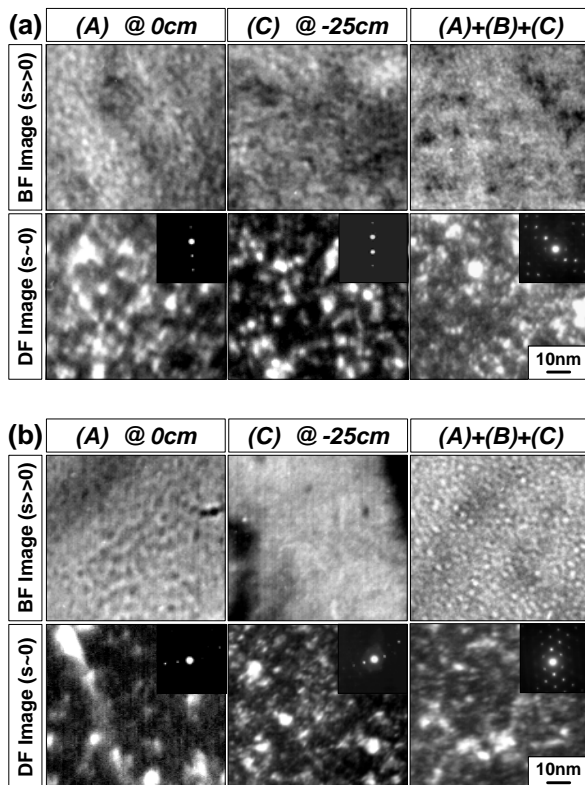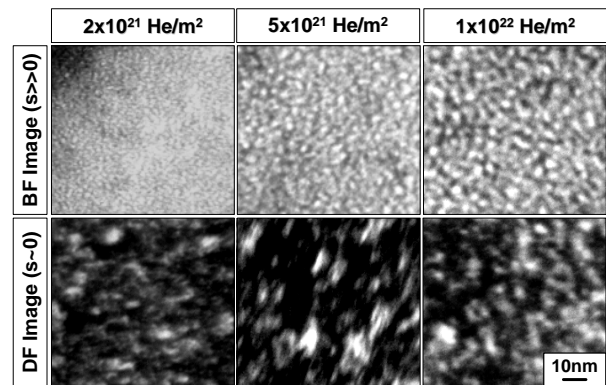
Fig.3 Microstructural evolution in stainless steel during helium ion irradiation ($\sim1\times10^{22}$ He/m^2) at room temperature with energies of 2 keV. BF images at large deviation parameter s (upper series). White dot contrast in DF images shows dislocation loops (lower series).

the case of only NBI heated helium discharges, very similar damages were confirmed after exposed to only ~100 s discharges in Mo and stainless steels specimens (not shown here). In the case of 2 keV-He$^+$, it was reported that at a dose level of lower than $\sim10^{20}$ He/m^{2}s, injected helium atoms are trapped by vacancy-helium complex and helium bubbles and finally filled with them. Above this dose level, additional trapping of helium atoms by helium bubbles become difficult [13].

Three-dimensional simulation of CX-neutral flux to the plasma facing components (whole torus wall ~300 m^2) during hydrogen discharge case in LHD as a function of line averaged electron density is under going now by using EMC3-EIRENE code (The calculation in helium discharge case is also under going). It is expected that more detailed analysis will be performed by comparing simulation results with experimental results.

3.3. Change of optical reflectivity

Fig. 4 shows the optical reflectivity of Mo specimen after exposed to NBI+ICRF heated helium discharges. This spectrum is from the specimen exposed to all position, (A)+(B)+(C) in table 1.

Reflectivity of virgin specimen was also plotted. It is clear that reduction of reflectivity has already occurred at the exposure time of only 1138 s. In particular, reduction of reflectivity about 500 nm or less is remarkable. Referring to our previous study [12], it is considered that reduction of optical reflectivity is due to the multiple scattering of light by the dense helium bubbles in the sub-surface region. In comparison with hydrogen irradiation, remarkable degradation of the optical reflectivity induced by hydrogen ions irradiation with similar energy occurs at the fluence above 10^{25}ions/m^2 [9]. We should note that effect of helium bombardment is three orders of magnitude higher than that of hydrogen bombardment. This result is important for the design and

Fig. 2 TEM images of (a)-Mo and (b)-stainless steel specimens after exposed to ICRF heated helium discharges, BF images at large deviation parameter s (upper series). White dot contrast in DF images shows dislocation loops (lower series).

for elucidation of the CX-particle load to first walls. Also

operation of plasma diagnostics using first mirror.
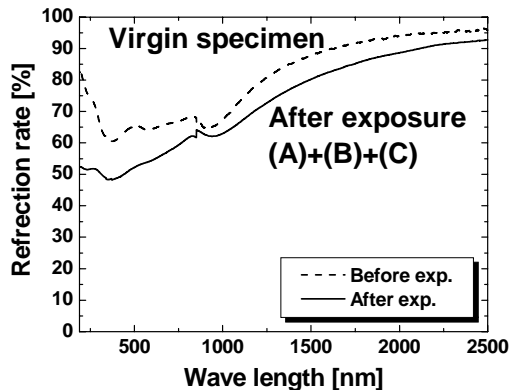
Fig.4 Optical reflectivity of Mo specimen after exposed to ICRF heated helium discharges. Solid line shows (A)+(B)+(C) in table 1. Dashed line shows virgin specimen.

4. Summary

Microscopic damages in metals bombarded by CX-helium atoms in LHD were observed by TEM, and the incident flux and energy of CX-helium particles to the first wall was discussed by comparing the microscopic damage properties with in-situ helium ion-beam irradiation experiment in laboratory. Dislocation loops and dense fine helium bubbles were formed in Mo and stainless steel specimens exposed only 349 s~1138 s to helium plasma discharges. It is considered that they are formed mainly by the bombardment of CX- helium atoms. The estimated flux and incident energy from size and density of the defects is the order of 2×10^{18}~1×10^{19} He/m^{2}s, and about 1~2keV, respectively.

Optical reflectivity of Mo specimen after exposed to NBI+ICRF heated helium discharges was measured by spectrophotometer. Reduction of reflectivity has already occurred at the exposure time of only 1138s. It is consider that reduction of optical reflectivity is due to the multiple scattering of light by the dense helium bubbles in the sub-surface region.

Generation of such high flux and high energy CX-helium atoms is serious problem for not only the deterioration of the first wall materials but also plasma diagnosis using metallic mirrors. In addition, phenomena in plasma confinement devices such as synergistic effects of helium bombardment and re-deposition will be investigated.

References

[1] R.J. Goldston, P.H. Rutherford, 1996 Introduction to Plasma Phys. p156
[2] H. Iwakiri et al., J. Nucl. Mater. 283-287 (2000) 1134
[3] N. Yoshida Y. Hirooka et a., J. Nucl. Mater. 258-263
[4] K. Ono et al., J. Nucl. Mater. 283-287 (2000) 210
[5] D. Nishijima et al., J. Nucl. Mater. 313-316 (2003) 97
[6] D. Nishijima et al., J. Nucl. Mater. 337-339 (2005) 927
[7] O. Motojima et al., 2003 Nucl. Fusion 43 1674
[8] A.E. Costley et al., Fusion Eng. Des. 55 (2001) 331
[9] V.S. Voitsenya et al., J. Nucl. Mater. 258-263 (1998) 1919
[10] V.S. Voitsenya et al., J. Nucl. Mater. 290-293 (2001) 336
[11] T. Sugie et al., J. Nucl. Mater. 329-333 (2004) 1481
[12] A. Ebihara et al., J. Nucl. Mater. 363-365 (2007) 1195
[13] M. Tokitani et al., J. Nucl. Mater. 329–333 (2004) 761